Regression Modeling and Process Analysis of Resistance Spot Welding on Dissimilar Steel Sheets

Fouad Ternane
Department of Mechanical Engineering
IS2M Laboratory, University of Aboubekr Belkaid
Tlemcen, Algeria
fouadsciences@yahoo.fr

Mustapha Benachour
Department of Mechanical Engineering
IS2M Laboratory, University of Aboubekr Belkaid
Tlemcen, Algeria
bmf_12002@yahoo.fr

Fethi Sebaa
Department of Mechanical Engineering
IS2M Laboratory, University of Aboubekr Belkaid
Tlemcen, Algeria
sebaafethi@yahoo.fr

Nadjia Benachour
Department of Mechanical Engineering
IS2M Laboratory, University of Aboubekr Belkaid
Tlemcen, Algeria

nbenachour2005@yahoo.fr

Received: 10 May 2022 | Revised: 27 May 2022 | Accepted: 28 May 2022

Abstract-The resistance spot welding process is used to weld dissimilar materials. Dissimilar joining is formed by two 2mm thick sheet metals of 304L austenitic stainless steel and galvanized steel. This study investigates the effects of welding parameters such as welding current, welding time, and welding force. The welding time and the welding force were, respectively, in the range of 10-13 cycles and 7-8bar, while the welding current was in the range of 10–16kA. Tensile tests were applied to determine the resistance parameters of dissimilar joining. The experimental results showed that increasing the welding current increased the tensile shear stress of the weld coupon. Regression analysis was carried out to determine the significance of the process parameters by using the coupled of the full factorial experimental design with statistical and graphical analysis of the results. Furthermore, analysis of variance was used to determine the optimal parameters and combinations to achieve the highest strength level.

Keywords-resistance spot welding; dissimilar joining; stainless steel & galvanized steel; welding parameters; regression model; tensile shear stress

I. INTRODUCTION

Resistance Spot Welding (RSW) is the main welding process used in the manufacturing industry, especially in the manufacturing of automobile truck cabins, rail vehicles, motorcycles, and home appliances such as refrigerators. For example, there are 3000 to 12000 spot welds in a car [1, 2]. The majority of the research investigations in spot welding has been carried out on the joining of homogeneous materials [3-6]. Currently, research in different industries is directed towards the reduction of CO_2 emissions. The combination of heterogeneous materials is necessary to reduce the weight of the structures and CO_2 emissions [7-9]. Engineers are increasingly looking to join different material types ensuring good mechanical strength, corrosion resistance, and sealing function [10, 11]. RSW of dissimilar materials was investigated in [10], finding that the lap shear strength depends on the strength and thickness of the non-stainless steels. A failure in dissimilar joining is called a plug failure.

The properties of RSW of dissimilar stainless steel lap joints were studied in [12], where the weld quality of dissimilar joints was linked to their tensile-shear strength. The welding current was the main governing factor that affected the tensile-shear strength of the RSW specimens. The current contribution of the weld was approximately 67% compared to weld time and applied load. As the weld current increases, the size of the weld nugget also increases. The mechanical performance of dissimilar stainless steel and carbon steel depends on the size of the fusion zone on the carbon steel side, where the pullout failure location of the carbon and stainless steel joint was in the Base Metal (BM) of the carbon steel side [11]. Tensile-shear properties and types of fracture of RSW joints were examined in [1], showing that increasing the weld time increased the tensile shear load-bearing capacity. Pullout and tearing failures are identified depending on the dissimilar joints (back hardening steel/304 stainless steel and back hardening steel/Interstitial steel). Pullout and interfacial failure modes were observed in several studies of homogeneous and inhomogeneous RSW of stainless steel and low carbon steel [11, 13-18]. The effects of welding current and welding process on residual stress distributions for dissimilar welded joints between stainless steel 316L and ferritic steel were investigated in [19], which have been used for lifetime assessment and failure mode predictions of the welded joints.

Several studies have been conducted to optimize the welding parameters [22-24]. Factorial analysis was applied to investigate the effect of feed water temperature, flow rate, and

Corresponding author: Fouad Ternane

radiator dimension on the total heat transfer coefficient and entropy generation in the panel radiator [22]. The effect of welding parameters on the tensile strength of RSW of the 5052Al alloy using a factorial design was studied in [25]. The effects of RSW process parameters and their interactions were studied in [26] using a non-linear regression model.

This paper presents an experimental study on determining the effect of the RSW parameters on the tensile-shear strength of dissimilar joints of stainless steel 304L with galvanized steel Z275. Linear regression, variance analysis, and a mathematical model were applied to evaluate the effects of the RSW parameters and some combinations on tensile-shear stress.

II. EXPERIMENTAL PROCEDURES

This study used 304L Stainless Steel (SS) and Z275 Galvanized Steel (GS), each having a thickness of 2mm. The chemical compositions of the steels are given in Table I. The dimensions of the tensile specimens were 85mm length and 30mm width, as shown in Figure 1. The total length of the RSW welded specimen was 140 mm.

TABLE I. CHEMICAL COMPOSITION OF THE WELDING MATERIALS

Element	C	Si	Mn	P	S	Cr	Ni
SS 304L	0.03	1.0	2.0	0.045	0.015	0.1	0.03
GS Z275	0.12	0.50	0.60	0.10	0.045	/	/

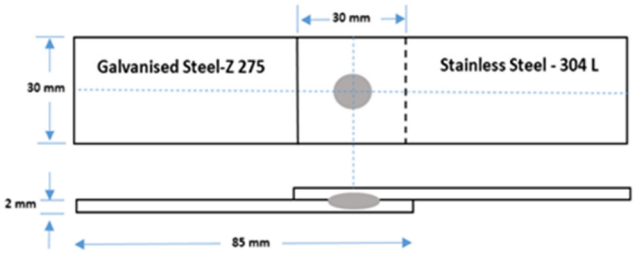

Fig. 1. Dimensions of the tensile test specimens.

The samples were welded by a TECNA ART 8201N RSW machine. Welding was performed using a water-cooled electrode with a hemispherical active face. The electrode in the $CuNi_2Be$ alloy had 6.0mm in contact surface according to:

$$D\ active = 2e + 3 \quad (1)$$

where D is the active diameter and e is the sheet thickness in mm.

III. WELDING PARAMETERS DETERMINATION

The welding parameters were determined from previous research and the weldability of materials, depending on the nature of the base materials and thickness [20]. The welding current varied from 10kA to 16kA, the welding time increased from 10 to 13 cycles, and two values of the electrode force (7 and 8bar) were also applied. The distribution of the values of the three parameters was carried out with a factorial plan to ensure the union of all the values. Table II shows the combination of the welding parameters and the number of trials for each factor. The mechanical properties of joining SS 304L and GS Z275 materials are given in Table III.

TABLE II. FACTORS OF WELDING PARAMETERS

Factor	Levels	Values
I (kA)	5	10; 12; 14; 15; 16
T (cycles)	3	10; 11; 13
F (bar)	2	7; 8

TABLE III. MECHANICAL PROPERTIES OF 304L SL AND Z275 GS

Materials	E (GPa)	σ_e(MPa)	UTS (MPa)	$A\%$	HRB
SS 304 L	190	336	655	43.2	60
GS Z275	200	266	330	22.0	/

IV. RESULTS AND DISCUSSION

A linear regression model was proposed to relate the tensile-shear strength of the RSW joints to welding current I, welding time T, and welding force F. Minitab 19 was used for regression analysis. As a result, a mathematical model was developed for the influence of the three welding parameters on tensile-shear stress, described as:

$$y = a + b1x1 + b2x2 + b3x3 + b11x1x1 + b23x2x3 \quad (2)$$

The regression equation between the welding parameters I, T, and F and tensile-shear strength was:

$$Tensile\ Shear\ Stress\ (MPa) = -343 + 33{,}2\,I + 35{,}4\,T + 47{,}4\,F - 0{,}767\,I^2 - 4{,}58\,T * F \quad (3)$$

Table IV shows the results of tensile-shear stress with the parameters of each test.

TABLE IV. EXPERIMENTAL DATA FOR TENSILE-SHEAR STRESS

Trial order	I (kA)	T (Cycles)	F (bar)	Tensile shear stress (MPa)
1	10	10	7	292.01
2	10	10	8	265.07
3	10	11	7	279.15
4	10	11	8	271.81
5	10	13	7	303.64
6	10	13	8	276.71
7	12	10	7	287.72
8	12	10	8	320.17
9	12	11	7	309.15
10	12	11	8	319.56
11	12	13	7	314.66
12	12	13	8	280.99
13	14	10	7	348.94
14	14	10	8	342.21
15	14	11	7	335.48
16	14	11	8	331.19
17	14	13	7	346.49
18	14	13	8	352.00
19	15	10	7	348.33
20	15	10	8	355.07
21	15	11	7	353.23
22	15	11	8	350.78
23	15	13	7	355.07
24	15	13	8	350.17
25	16	10	7	363.02
26	16	10	8	355.07
27	16	11	7	344.66
28	16	11	8	348.33
29	16	13	7	363.02
30	16	13	8	356.90

Table V illustrates the results of the analysis of variance with some interactions between the three welding parameters. The data show that the main effects of the welding current are relevant for the maximum load. Since the p-value of welding current is inferior to the significance level established at a 5% probability level (p<0.05), the interaction between welding time and electrode force cannot be considered significant. This Table also shows other adequacy measures: R^2=88.96%, adjusted R^2=86.66%, and predicted R^2=81.59%. Since they are all very close to 0.9, they indicate a suitable model.

TABLE V. ANALYSIS OF VARIANCE

Source	DF	Adj. SS	Adj. MS	F.Value	P.Value
Regression	5	25237.7	5047.5	38.68	0.000
I	1	632.6	632.6	4.85	0.038
T	1	258.8	258.8	1.98	0.172
F	1	201.3	201.3	1.54	0.226
*I*I*	1	228.4	228.4	1.75	0.198
*T*F*	1	245.0	245.0	1.88	0.183
Error	24	3132.0	130.5		
Total	29	28369.7			

R^2= 88.96%

Adjusted R^2 = 86.66%

Predicted R^2 = 81.59%

It is necessary to compare the tensile shear stress values estimated by the model equations (2), (3) with the values obtained as a result of experimental calculations. The residuals consist of the difference between the data and the model data. A comparison of the estimated and experimental data for tensile shear stress is shown in Figure 2 [26, 27]. According to Figure 2, a good agreement was observed between the mathematical model obtained for the tensile-shear stress and the experimental data, and residuals fall relatively along a straight line. Consequently, the normal distribution assumption was considered satisfied.

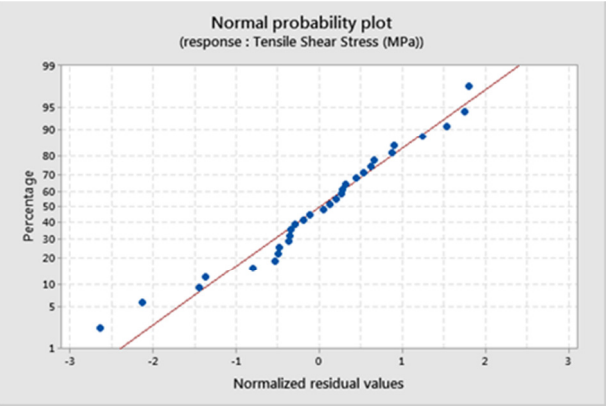

Fig. 2. Normal probability plot of residuals.

Figure 3 is a residual versus observation order graph showing that all residual points are spread within the lower and upper bounds without evident patterns, confirming the assumption that the residuals have a regular variance. As a result, all diagnostic plots denote that all the necessary ANOVA assumptions are satisfied.

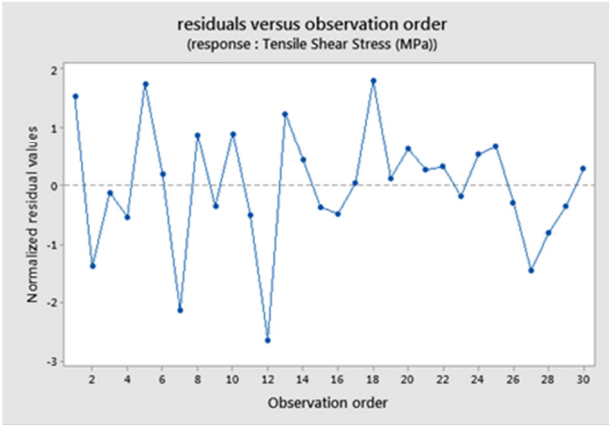

Fig. 3. Residuals versus observation order.

As shown in Figure 4, all residual points are dispersed within the lower and upper bounds, showing no pattern. This graph denotes that the independence assumption is also satisfied. The histogram shown in Figure 5 forms a normal curve equally distributed around zero, showing that the normality assumption is more than likely true.

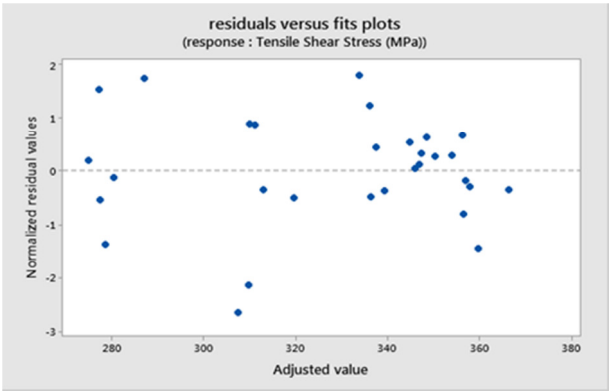

Fig. 4. Residuals versus fits plots.

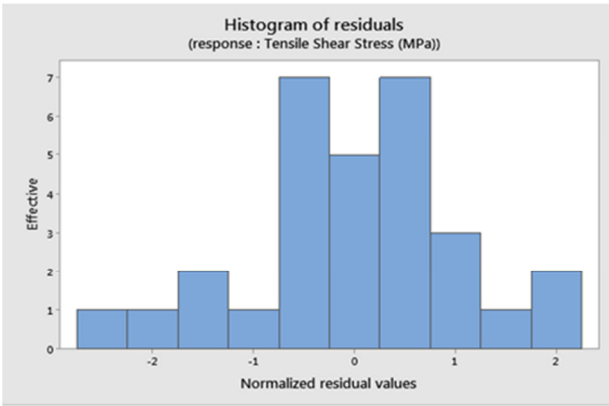

Fig. 5. Histogram of residuals.

As shown in Figure 6, a Pareto diagram provides statistical information on the effects of input variables, factors or welding parameters in this case, on tensile shear stress. It is observed that the welding current factor has a relevant impact on the

tensile-shear stress because it occurs outside the dotted line at 2.064. The other parameters and interactions have a meaningless or less impact relative to the welding current. It is important to know the effect levels of welding parameters on tensile-shear stress. Using this information, one could choose which parameter is more important for perfect welding joining [22, 28].

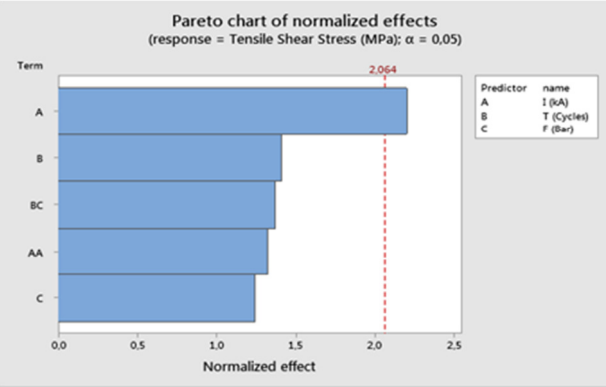

Fig. 6. Pareto chart of normalized effects.

These factors can be classified in decreasing order: welding time, welding time electrode force interaction, welding current, welding current interaction, and welding force. This result can be further supported by taking into account the main effects and interaction graphs, as shown in Figures 7 and 8 respectively. Figure 7 shows a graphical representation of the primary effects of the factors examined for the spot weld regarding tensile-shear stress. According to the graph, it can be concluded that the impact of a factor is directly linked to the slope and length of the line in the graphic. The greater the slope is, the higher the influence on the average maximum load increase will be when varying levels from low to high. According to Figure 7, the welding current has a significant impact on tensile-shear stress due to the higher slope, while welding time is less sensitive to the variability in tensile-shear stress compared to welding current. On the other hand, welding force has less effect on tensile shear stress.

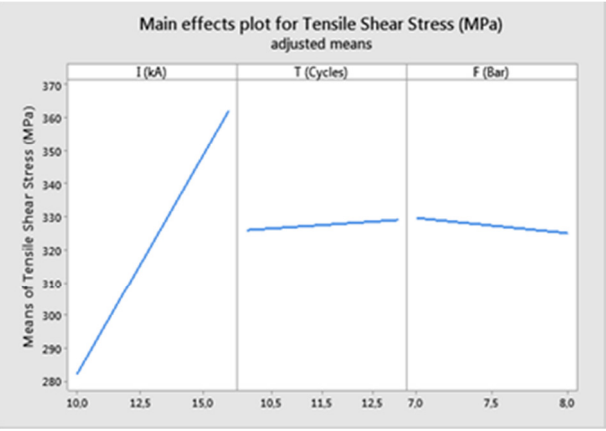

Fig. 7. Main effects plot for tensile shear stress (MPa).

Figure 8 shows the main effect graph for tensile-shear stress. The three two-factor interaction graphs denote a powerful interaction between welding current and welding time, and welding current and welding force. Tensile-shear stress reaches its highest when welding current and welding time are kept at a high level, but welding force is at a low level, 16kA, 13cycles, and 7bar respectively. Similarly, tensile-shear stress reaches its minimum when welding current and welding time are both at low levels, but electrode force maintains a high level, i.e. 10kA, 10cycles, and 8bar respectively.

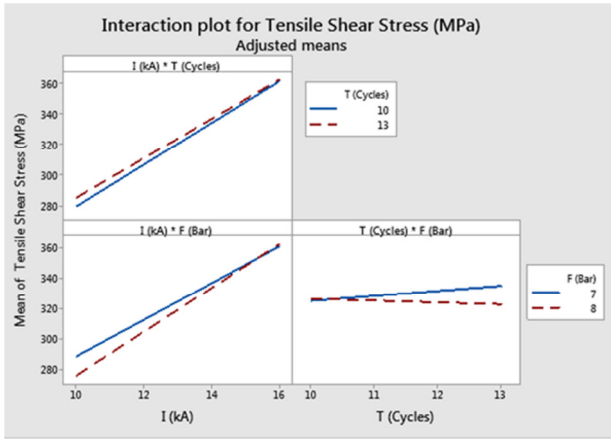

Fig. 8. Interaction plot for Tensile shear stress (MPa)

V. CONCLUSION

This paper presented a linear regression analysis used to investigate the effect of RSW parameters on the tensile-shear stress of dissimilar joints from experimental results. Based on this investigation, the following conclusions can be drawn:

- The regression analysis showed that there is a linear relationship between welding parameters (welding current, welding time, and electrode force) and the tensile-shear strength of the RSW joints.
- According to the p-values and the Pareto chart, the welding current had the highest impact on tensile-shear stress compared to welding time, welding force, and other combinations.
- The welding process and the effects of parameters and interactions between them on tensile-shear strength can be analyzed based on regression models of the welding process on two heterogeneous sheets, stainless steel and galvanized steel, with a thickness of 2mm which can make it to be an assistant reference for the welding process.
- The optimal parameters that gave a higher tensile-shear strength were higher welding current (16kA) and welding time (13cycles) and lower welding force (7bar).

ACKNOWLEDGMENT

The authors gratefully acknowledge the technical support and welding specimens from the SOREMEP Society in Tlemcen.

REFERENCES

[1] F. Hayat, "Resistance Spot Weldability of Dissimilar Materials: BH180-AISI304L Steels and BH180-IF7123 Steels," *Journal of Materials Science & Technology*, vol. 27, no. 11, pp. 1047–1058, Nov. 2011, https://doi.org/10.1016/S1005-0302(11)60185-0.

[2] M. R. A. Shawon, F. Gulshan, and A. S. W. Kurny, "Effect of Welding Current on the Structure and Properties of Resistance Spot Welded Dissimilar (Austenitic Stainless Steel and Low Carbon Steel) Metal Joints," *Journal of The Institution of Engineers (India): Series D*, vol. 96, no. 1, pp. 29–36, Apr. 2015, https://doi.org/10.1007/s40033-014-0060-6.

[3] A. Deliou and B. Bouchouicha, "Fatigue crack propagation in welded joints X70," *Frattura ed Integrità Strutturale*, vol. 12, no. 46, pp. 306–318, Sep. 2018, https://doi.org/10.3221/IGF-ESIS.46.28.

[4] B. Ahmed, O. C. E. Bahri, B. Benattou, and T. Malika, "Numerical Simulation of a Steel Weld Joint and Fracture Mechanics Study of a Compact Tension Specimen for Zones of Weld Joint," *Frattura ed Integrità Strutturale*, vol. 13, no. 47, pp. 17–29, 2019, https://doi.org/10.3221/IGF-ESIS.47.02.

[5] M. N. James and M. Newby, "The interface between metallurgy and mechanics in material performance," *Frattura ed Integrità Strutturale*, vol. 4, no. 14, pp. 5–16, 2010, https://doi.org/10.3221/IGF-ESIS.14.01.

[6] A. Alzahougi, M. Elitas, and B. Demir, "RSW Junctions of Advanced Automotive Sheet Steel by Using Different Electrode Pressures," *Engineering, Technology & Applied Science Research*, vol. 8, no. 5, pp. 3492–3495, Oct. 2018, https://doi.org/10.48084/etasr.2342.

[7] B. Mezrag, F. Deschaux-Beaume, and M. Benachour, "Control of mass and heat transfer for steel/aluminium joining using Cold Metal Transfer process," *Science and Technology of Welding and Joining*, vol. 20, no. 3, pp. 189–198, Mar. 2015, https://doi.org/10.1179/1362171814Y.0000000271.

[8] A. O. İrizalp, H. Durmuş, N. Yüksel, and İ. Türkmen, "Cold metal transfer welding of AA1050 aluminum thin sheets," *Matéria (Rio de Janeiro)*, vol. 21, pp. 615–622, Sep. 2016, https://doi.org/10.1590/S1517-707620160003.0059.

[9] A. Subrammanian, D. B. Jabaraj, and V. K. Bupesh Raja, "Investigation of Microstructure and Mechanical Properties of Resistance Spot Welded Dissimilar Joints Between Ferritic Stainless Steel and Weathering Steel," *Applied Mechanics and Materials*, vol. 766–767, pp. 770–779, 2015, https://doi.org/10.4028/www.scientific.net/AMM.766-767.770.

[10] M. Alenius, P. Pohjanne, M. Somervuori, and H. Hänninen, "Exploring the mechanical properties of spot welded dissimilar joints for stainless and galvanized steels," *Welding Journal*, vol. 85, no. 12, pp. 305–313, 2006.

[11] M. Pouranvari and S. P. H. Marashi, "Similar and dissimilar RSW of low carbon and austenitic stainless steels: effect of weld microstructure and hardness profile on failure mode," *Materials Science and Technology*, vol. 25, no. 12, pp. 1411–1416, Dec. 2009, https://doi.org/10.1179/026708309X12459430509292.

[12] A. B. Verma, S. U. Ghunage, and B. B. Ahuja, "Resistance Welding of Austenitic Stainless Steels (AISI 304 with AISI 316)," presented at the 5th International & 26th All India Manufacturing Technology, Design and Research Conference (AIMTDR 2014), Guwahati, India, Dec. 2014.

[13] A. M. Pereira, J. M. Ferreira, A. Loureiro, J. D. M. Costa, and P. J. Bártolo, "Effect of process parameters on the strength of resistance spot welds in 6082-T6 aluminium alloy," *Materials & Design (1980-2015)*, vol. 31, no. 5, pp. 2454–2463, May 2010, https://doi.org/10.1016/j.matdes.2009.11.052.

[14] M. Pouranvari, S. M. Mousavizadeh, S. P. H. Marashi, M. Goodarzi, and M. Ghorbani, "Influence of fusion zone size and failure mode on mechanical performance of dissimilar resistance spot welds of AISI 1008 low carbon steel and DP600 advanced high strength steel," *Materials & Design*, vol. 32, no. 3, pp. 1390–1398, Mar. 2011, https://doi.org/10.1016/j.matdes.2010.09.010.

[15] M. Elitas and B. Demir, "The Effects of the Welding Parameters on Tensile Properties of RSW Junctions of DP1000 Sheet Steel," *Engineering, Technology & Applied Science Research*, vol. 8, no. 4, pp. 3116–3120, Aug. 2018, https://doi.org/10.48084/etasr.2115.

[16] F. Nikoosohbat, S. Kheirandish, M. Goodarzi, M. Pouranvari, and S. P. H. Marashi, "Microstructure and failure behaviour of resistance spot welded DP980 dual phase steel," *Materials Science and Technology*, vol. 26, no. 6, pp. 738–744, Jun. 2010, https://doi.org/10.1179/174328409X414995.

[17] M. Ishak, L. H. Shah, I. S. R. Aisha, W. Hafizi, and M. R. Islam, "Study of Resistance Spot Welding Between AISI 301 Stainless Steel and AISI 1020 Carbon Steel Dissimilar Alloys," *Journal of Mechanical Engineering and Sciences*, vol. 6, pp. 793–806, Jun. 2014, https://doi.org/10.15282/jmes.7.2014.7.0077.

[18] M. Safari and H. Mostaan, "Dissimilar resistance spot welding of AISI 1075 eutectoid steel to AISI 201 stainless steel," *Journal of Advanced Materials and Processing*, vol. 5, no. 1, pp. 44–56, Mar. 2017.

[19] R. Konecná, L. Kunz, G. Nicoletto, and A. Baca, "Fatigue crack growth behavior of Inconel 718 produced by selective laser melting," *Frattura ed Integrità Strutturale*, vol. 10, no. 35, pp. 31–40, 2016, https://doi.org/10.3221/IGF-ESIS.35.04.

[20] M. Pouranvari, P. Marashi, and M. Goodarzi, "Failure Mode of Dissimilar Resistance Spot Welds Between Austenitic Stainless and Low Carbon Steels," in *Proceedings of Metal 2008*, Hradec nad Moravicí, Czech Republic, May 2008.

[21] P. Russo Spena, M. De Maddis, F. Lombardi, and M. Rossini, "Dissimilar Resistance Spot Welding of Q&P and TWIP Steel Sheets," *Materials and Manufacturing Processes*, vol. 31, no. 3, pp. 291–299, Feb. 2016, https://doi.org/10.1080/10426914.2015.1048476.

[22] K. Gelis, "Factorial experimental design for second law analysis of panel radiators as a function of radiator dimension," *Journal of Building Engineering*, vol. 43, Nov. 2021, Art. no. 102872, https://doi.org/10.1016/j.jobe.2021.102872.

[23] J. Valera, V. Miguel, A. Martínez, J. Naranjo, and M. Cañas, "Optimization of electrical parameters in Resistance Spot Welding of dissimilar joints of micro-alloyed steels TRIP sheets," *Procedia Manufacturing*, vol. 13, pp. 291–298, Jan. 2017, https://doi.org/10.1016/j.promfg.2017.09.074.

[24] V. C. Nguyen, T. D. Nguyen, and D. H. Tien, "Cutting Parameter Optimization in Finishing Milling of Ti-6Al-4V Titanium Alloy under MQL Condition using TOPSIS and ANOVA Analysis," *Engineering, Technology & Applied Science Research*, vol. 11, no. 1, pp. 6775–6780, Feb. 2021, https://doi.org/10.48084/etasr.4015.

[25] P. Peasura, "Optimization of Resistance Spot Welding on Aluminum Magnesium 5052 Grade with 23 Factorial Designs," *Advanced Materials Research*, vol. 622–623, pp. 340–343, 2013, https://doi.org/10.4028/www.scientific.net/AMR.622-623.340.

[26] Y. Luo, J. Liu, H. Xu, C. Xiong, and L. Liu, "Regression modeling and process analysis of resistance spot welding on galvanized steel sheet," *Materials & Design*, vol. 30, no. 7, pp. 2547–2555, Aug. 2009, https://doi.org/10.1016/j.matdes.2008.09.031.

[27] S. M. Hamidinejad, F. Kolahan, and A. H. Kokabi, "The modeling and process analysis of resistance spot welding on galvanized steel sheets used in car body manufacturing," *Materials & Design*, vol. 34, pp. 759–767, Feb. 2012, https://doi.org/10.1016/j.matdes.2011.06.064.

[28] T. Saeheaw, "Regression Modeling and Process Analysis of Plug and Spot Welds Used in Automotive Body Panel Assembly," *International Journal of Engineering*, vol. 33, no. 11, pp. 2384–2398, Nov. 2020, https://doi.org/10.5829/ije.2020.33.11b.29.